

# Green Chemistry

Accepted Manuscript



This article can be cited before page numbers have been issued, to do this please use: P. Losch, J. F. KOLB, A. ASTAFAN, T. J. Daou, L. Pinard, P. Pale and B. Louis, *Green Chem.*, 2016, DOI: 10.1039/C6GC00731G.



This is an *Accepted Manuscript*, which has been through the Royal Society of Chemistry peer review process and has been accepted for publication.

*Accepted Manuscripts* are published online shortly after acceptance, before technical editing, formatting and proof reading. Using this free service, authors can make their results available to the community, in citable form, before we publish the edited article. We will replace this *Accepted Manuscript* with the edited and formatted *Advance Article* as soon as it is available.

You can find more information about *Accepted Manuscripts* in the [Information for Authors](#).

Please note that technical editing may introduce minor changes to the text and/or graphics, which may alter content. The journal's standard [Terms & Conditions](#) and the [Ethical guidelines](#) still apply. In no event shall the Royal Society of Chemistry be held responsible for any errors or omissions in this *Accepted Manuscript* or any consequences arising from the use of any information it contains.

## Eco-Compatible Zeolite-Catalysed Continuous Halogenation of Aromatics

P. Losch,<sup>a</sup> J. F. Kolb,<sup>a</sup> A. Astafan,<sup>b,c</sup> T. J. Daou,<sup>b,\*</sup> L. Pinard,<sup>c</sup> P. Pale,<sup>a</sup> B. Louis<sup>a,\*</sup>

*a) Laboratoire de Synthèse Réactivité Organiques et Catalyse (LASYROC), UMR 7177, Institut de Chimie, Université de Strasbourg, 1 rue Blaise Pascal, 67000 Strasbourg Cedex, France. E-mail: blouis@unistra.fr*

*b) Université de Haute Alsace (UHA), CNRS, Equipe Matériaux à Porosité Contrôlée (MPC), Institut de Science des Matériaux de Mulhouse (IS2M) UMR 7361, ENSCMu, Mulhouse Cedex 68093, France. E-mail: jean.daou@uha.fr*

*c) Institut de Chimie des Milieux et Matériaux de Poitiers, UMR 7285 CNRS, 4 Rue Michel Brunet, Bâtiment B27, 86073 Poitiers Cedex9 France.*

### Abstract

A completely eco-compatible halogenation reaction of arenes has been developed allowing high conversions (> 95 %) of iodobenzene with nearly 100 kg iodobenzene converted per kg<sub>cat</sub> in one day. Several solid acids, zeolites being the most promising, have been successfully tested in the chlorination reaction of iodobenzene by trichloroisocyanuric acid (TCCA), a green chlorination agent. H-\*BEA zeolites were found to be the most active catalysts for this model halogenation reaction. A strong structure-activity relationship could be established thanks to various synthetic zeolites and corresponding thorough characterisation (SEM, BET, XRD, FTIR). Indeed, nano-sized \*BEA zeolites and more specifically nanosponge-like \*BEA crystals exhibited the highest catalytic performance with a conversion up to 100% and a selectivity toward monochlorinated products up to 98 %.

Finally, the gained knowledge was applied to set-up an eco-compatible continuous flow halogenation process of different aromatics catalysed by H-\*BEA zeolites.

*Keywords: chlorination, BEA zeolite, acid catalysis, nanosponge, flow-chemistry.*

## 1. Introduction

Halogenation of arenes leads to valuable starting molecules in fine chemistry as an entry towards the synthesis of dyes, bio-active compounds such as pesticides or pharmaceuticals.<sup>1</sup> This generally Lewis acid catalysed reaction is known since the 1950's and most commonly involves  $\text{FeCl}_3$  as a catalyst.<sup>2</sup> Nowadays, it is implemented in industry at the megaton-scale and still facing an annual growth demand of roughly 5%.<sup>3</sup> It is of paramount importance to underline the ongoing progress in sustainable arene production complementing classical unsustainable resources, for instance biomass-derived dimethylfuran (DMF) and bioethanol to renewable xylene.<sup>4</sup>

Unfortunately, industrial methods for the most commonly used aromatics halogenation reactions usually produce mixtures of regioisomers, difficult to separate, thus raising the production cost.<sup>5</sup> Notably, the Raschig-Hooker process has been industrially applied for a long time to produce chlorobenzene and phenol in a continuous flow process with hydrochloric acid and *in situ* generation of  $\text{Cl}_2$  gas using a  $\text{CuCl-CuCl}_2$  mixed catalyst.<sup>6</sup> Another drawback relies on the use of corrosive acid catalysts such as Lewis acids (aluminum chloride or boron trifluoride), used in (super)stoichiometric amounts and which are consumed during the course of the reaction. Likewise, strong Brønsted acid catalysts such as sulphuric acid remain very corrosive and generate high amounts of salts as by-products.

Recently, the scientific community focused on developing more efficient and selective processes for the halogenation of arenes.<sup>7</sup> For instance, de Mattos *et al.* developed a methodology for the halogenation of deactivated arenes using trichloro- / trihaloisocyanuric acid (TC(Hal)CA) in a superelectrophilic medium (Figure 1).<sup>8</sup> TCCA is a stable and inexpensive solid, easily available in pool supplies, commonly used as swimming-pool disinfectant and bleaching agent. It is an efficient chlorine source due to its highly electrophilic chlorine content and has already been used in numerous chlorination reactions of diverse organic compounds as well as in oxidation reactions.<sup>9,10</sup>

These early studies have been carried out in homogeneous superacidic conditions, while the green chemistry principle of catalysis, encompassing both homogeneous and heterogeneous catalysis, is becoming increasingly ubiquitous in organic chemistry. Heterogeneous catalysts are easily adopted in gas-solid or liquid-solid flow processes; thereby they may allow to continuously produce high-value added chemicals.<sup>11</sup> In heterogeneously catalysed reactions, the key solid acid catalysts in petrochemistry, and increasingly in biomass reforming processes, remain zeolites.<sup>12</sup> In addition, to their three-dimensional crystalline microporous network, zeolites are characterised by a strong acidity. Those (often) synergetic properties led them to exhibit high conversions and excellent selectivities in many targeted reactions either in petrochemical processes but in more complex reactions as well, for instance biomass conversion.<sup>13,14</sup> Smith *et al.* highlighted the advantages and limitations of zeolites uses in electrophilic aromatic substitutions, leading, in general, to higher *para*-selectivities.<sup>15</sup>

Our group recently transposed batch conditions for activated aromatics (toluene, anisole) to gas phase semi-continuous flow operations for the chlorination of activated and deactivated arenes (toluene, chlorobenzene and nitrobenzene).<sup>16</sup> An interesting conclusion of this work was the correlation between the zeolite pore topologies and their ability to convert variously substituted aromatics. Indeed, an optimal activity for the following couples has been reported: H-USY - nitrobenzene, H-ZSM-5 - chlorobenzene and H-ZSM-5 - toluene.<sup>16</sup> Although this process already avoids the use of toxic or volatile solvents and gaseous chlorine, we have to state the remaining downsides consisting in a generally low productivity and relatively high reaction temperatures. Furthermore, the sole fact that the operation was in a semi-continuous mode further hampers the process viability. Nevertheless, these pioneering studies are pointing towards the way to design a truly eco-compatible and competitive halogenation process (Figure 1, step 5).

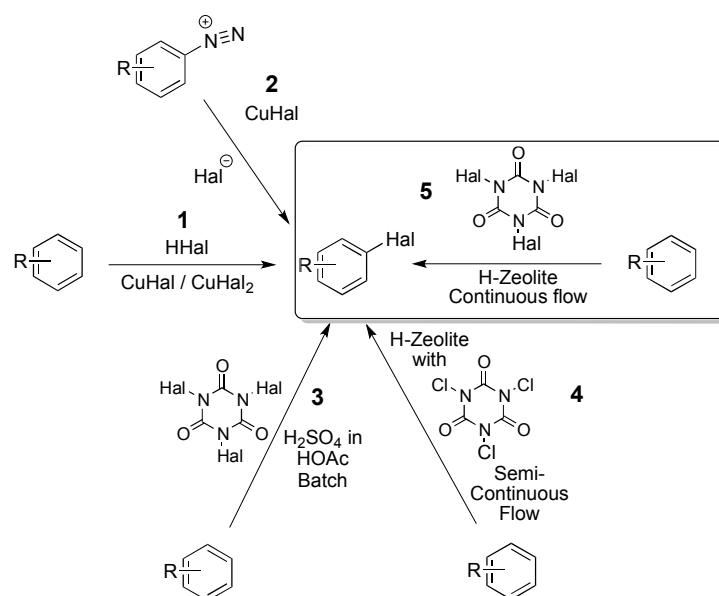


**Figure 1.** Different reaction pathways to produce halogenated aromatics 1) Raschig-Hooker process,<sup>6</sup> 2) Sandmeyer reaction, 3) T(Hal)CA in superelectrophilic medium,<sup>7,8</sup> 4) Semi-continuous chlorination reaction,<sup>16</sup> 5) Heterogeneous continuous flow process presented herein.

In the present work, we report the screening of heterogeneous catalysts for converting iodobenzene into monochlorinated chloriodobenzenes using trichloroisocyanuric acid (TCCA) as chlorination agent. This reaction was chosen as a benchmark reaction for the optimisation of reaction conditions. Nevertheless, its intrinsic interest is not negligible, because chloriodobenzenes (High value added chemicals cf. Table S1) are used in polymer chemistry,<sup>17</sup> and in stepwise C-C coupling reactions.<sup>18</sup> However, the latter molecules are still produced with gaseous chlorine over  $\text{AlCl}_3$ ,  $\text{FeCl}_3$  or  $\text{SbCl}_5$  catalysts.<sup>19,20</sup> Then, once optimised conditions could be set up towards an eco-compatible

halogenation of variously substituted arenes in a batch reactor. Ultimately, we report a transposition attempt to develop a continuous flow liquid-solid process.

## 2. Experimental

### 2.1 Catalyst preparation

Homogeneous catalysts, tested for comparison, were sulphuric acid (Aldrich, 98%) and aluminum trichloride (Aldrich, > 99.0%) and were used as received.

Three different \*BEA zeolites were synthesised and named hereafter \*BEA-MC (**MC**) for microcrystals, \*BEA-NC (**NC**) for nanocrystals and \*BEA-NS (**NS**) for nanosponges. The procedures applied to obtain those materials are described in the S.I. and were recently reported by Astafan *et al.*<sup>21</sup>

The H-forms of **MC**, **NC** and **NS** zeolites were obtained by double ion exchange of calcined zeolite with a 1M NH<sub>4</sub>NO<sub>3</sub> solution (liquid/solid ratio: 20 mL.g<sup>-1</sup>) at 80°C for 1h and calcination in a static oven at 550°C for 5h.

### 2.2 Catalyst characterisation

The crystallinity and purity of as-synthesised materials were checked by powder X-ray diffraction (XRD) on a PANalytical MPD X'Pert Pro diffractometer operating with Cu K $\alpha$  radiation ( $\lambda$  = 0.15418 nm) and equipped with an X'Celerator real-time multiple strip detector (active length = 2.122° 2 $\theta$ ). The powder pattern was collected at room temperature in the range 3 < 2 $\theta$  < 50° with a 2 $\theta$  angle step of 0.017° and a step time of 220s. Small angle powder X-ray diffraction patterns in the 0.5-10° region were recorded on a glass plate with a 0.02° step size (step time = 1s) and a variable slit mode. The morphology, homogeneity and particle sizes of the samples were investigated with a scanning electron microscope (SEM) (Philips XL30 FEG) and by transmission electron microscopy (TEM) using a Philips model CM200, under an acceleration voltage of 200 kV, with a point-to-point resolution of 0.3 nm.

The Si/Al molar ratios were determined by X-Ray Fluorescence spectrometry (Philips, Magic X). The Al zeolite framework (Al<sub>Fram</sub>) content was determined by infrared spectroscopy measurements on a FT-IR Magna 550 Nicolet spectrometer. The position of the zeolite structural bands (450-1250 cm<sup>-1</sup>) and especially that of the asymmetric stretch vibration at 1080-1200 cm<sup>-1</sup> allows estimating the Al<sub>Fram</sub> from the correlation given in literature.<sup>22</sup> The TOT bands were determined using KBr wafers containing 2 wt % of sample.

Home-made H/D isotope exchange technique was used to determine the number of Brønsted acid sites present in the different solid acids.<sup>23</sup>

A Micromeritics 2420 ASAP was used for nitrogen sorption measurements. Prior to each experiment, 50 mg of the calcined zeolite samples were outgassed to a residual pressure of less than 0.8 Pa at 300°C for 15h. Nitrogen sorption measurements were performed at -196°C. Specific surface areas were determined from the Brunauer-Emmet-Teller (BET) equation in the  $p/p_0$  range between 0.05 and 0.25. The total pore volume was determined from the nitrogen adsorbed volume at  $p/p_0 = 0.99$  and the  $t$ -plot method was used to distinguish micropores from mesopores.

Infrared spectra (FT-IR) of pyridine (Py) adsorbed at 100°C were recorded on a Nicolet Magna 550 FT-IR spectrometer with a 2  $\text{cm}^{-1}$  optical resolution. After establishing a pressure of 1 Torr at equilibrium, the cell was evacuated at 150°C to remove all physisorbed species. The amounts of pyridine adsorbed on the Brønsted [ $\text{PyH}^+$ ] and Lewis [ $\text{PyL}$ ] sites were determined from the integration of the band at 1545 and 1454  $\text{cm}^{-1}$ , using extinction coefficients previously determined.<sup>24</sup>

The textural and acidic properties characterised by H/D isotopic exchange of commercially available materials are listed in Table 1.

**Table 1.** Characterisation of the different commercial solid acid catalysts.

Entry	Catalyst	Si/Al	$n(\text{H}^+)$ [mmolH <sup>+</sup> /g <sub>cat</sub> ] <sup>a</sup>	$S_{\text{BET}}$ [m <sup>2</sup> .g <sup>-1</sup> ]	Pore size [Å]	Crystal size [nm]
1	ZSM-5 (Zeolyst CBV2314)	13	1.48	425	5.5	< 100
2	ZSM-5 (Zeolyst CBV5524)	25	0.86	425	5.5	< 100
3	MOR (Zeolyst )	10	1.90	550	7	1000 - 1500
4	USY (Zeolyst)	3.6	3.80	750	12	500-700
5	Y (Aldrich)	2.2	5.37	710	12	500-800
6	EMT (UOP)	6.5	2.38	631	12	2000
7	Cs <sub>2</sub> HPW <sub>12</sub> O <sub>40</sub>	-	0.32	123	-	1000-2000
8	*BEA (Zeochem)	14	1.07	620	6 <sup>b</sup>	100 - 400

<sup>a</sup> Acid site densities are obtained by H/D-isotope exchange ; <sup>b</sup> Precise pore dimensions for \*BEA micropores: 6.6 x 6.7 and 5.6 x 5.6 Å.

### 2.3 Catalytic testing

**Classic batch conditions.** Catalytic reactions were initially carried out in 5 mL dichloroethane, to which iodobenzene (1 mmol, 0.112 mL, 1 equiv.), TCCA (0.34 mmol, 0.079 g, 0.34 equiv.) and the respective heterogeneous catalyst (100 mg) were added (isomass conditions were chosen). The solution was stirred at 80°C and 500 rpm velocity (a yellow coloration was observed). The samples withdrawn for GC analysis were treated to neutralise residual TCCA,  $\text{Cl}^0$  - or  $\text{Cl}^{+x}$  species. Namely, 0.1 mL of the reaction mixture was filtered over a celite filled cartridge with 2 mL  $\text{CH}_2\text{Cl}_2$  and vigorously stirred with 3 mL of a 10 wt-%  $\text{Na}_2\text{S}_2\text{O}_3$  solution. From the resulting biphasic solution, the organic layer was separated and dried over  $\text{Na}_2\text{SO}_4$  and finally injected in the gas

chromatograph (GC II 5890 Hewlett Packard) equipped with a capillary column (PONA, 50 m) and a flame ionisation detector (FID). A typical chromatogram and integration results are given in S.I. (Figures S1 and S2).

In principle, the chlorination of iodobenzene leads to mono-, di- or tri-substituted aromatics. *Para*- and *ortho*-substituted aromatics are favoured. The degree of conversion and the selectivity toward the different products were calculated by taking into account the response factors from the reagent iodobenzene and those from the products (mono-, di- and tri-chlorinated aromatics) through the use of an external standard (n-heptane). For the different reaction conditions, different substrates and solvents were needed for the interpretation of GC results in order to determine conversions and selectivities. They were realised by adding the substrate (1 mmol), dichloroethane (0.08 mL, as internal standard) to 5 mL of solvent. 0.1 mL were extracted and mixed with 2 mL of EtOAc. The solution was injected three times in the gas chromatograph.

Then, blank experiments were carried out without catalyst and with two homogeneous catalysts : sulphuric acid and aluminum trichloride, tested under iso-site conditions with respect to 100 mg H-ZSM-5 zeolyst CBV2314, ergo 0.148 mmol H<sup>+</sup> or Al which corresponded to; 8  $\mu$ L H<sub>2</sub>SO<sub>4</sub> and 20 mg AlCl<sub>3</sub>. Besides, different solvents (5 mL) were tested in the benchmark reaction with iodobenzene (1 mmol, 0.112 mL, 1 eq.), TCCA (0.34 mmol, 0.079 g, 0.34 equiv) and commercial \*BEA zeolite (100 mg).

After replacing hazardous solvents (Table 4), the scope of \*BEA-catalysed halogenation reactions was evaluated by testing different halogenating agents: N-chlorosuccinimide (NCS, Aldrich, 99%), N-bromosuccinimide (NBS, Aldrich, 99%) and N-iodosuccinimide (NIS, Alfa Aesar, 99%).

Two different kinds of operations were applied as following:

**a) Batch conditions (optimised).** Reactions were carried out in 5 mL acetic acid, aromatic substrate (1 mmol, 1 eq.), TCCA (0.34 mmol, 0.079 g, 0.34 equiv), dichloroethane (1 mmol, 0.08 mL) as an internal standard for GC analysis and \*BEA (100 mg) were added (isomass conditions). The solution was stirred at 80°C and 500 rpm velocity (a pale yellow coloration was observed). The samples withdrawn for GC analysis were treated to neutralise residual TCCA, acetic acid, Cl<sup>0</sup> - or Cl<sup>+x</sup> - species. Namely, 0.1 mL of the reaction mixture was filtered over celite filled cartridge with 2 mL EtOAc and vigorously stirred with 3 mL of a 10 %wt. K<sub>2</sub>CO<sub>3</sub> solution. From the resulting biphasic solution, the organic layer was separated and dried over Na<sub>2</sub>SO<sub>4</sub> and finally injected in the gas chromatograph (GC II 5890 Hewlett Packard) equipped with a flame ionisation detector (FID).

**b) Continuous flow.** A glass U-shaped tubular reactor (Figure 2) was used in a continuous flow chlorination operation. The reactants TCCA (316 mg, 1.36 mmol), iodobenzene (0.448 mL, 4 mmol) and dichloroethane as an internal standard (0.32 mL, 4 mmol) were previously solubilised in acetic acid and charged into a 20 mL syringe. The U-shaped glass reactor was packed with 33 mg of respective \*BEA zeolite. Those loadings were chosen to set the same contact time corresponding to 12 consecutive runs under batch conditions.

Recycling was tested; solid catalysts were re-engaged up to ten times after centrifugation and washing three times with 5 mL H<sub>2</sub>O/EtOH (50/50). No re-activation was needed between consecutive runs.

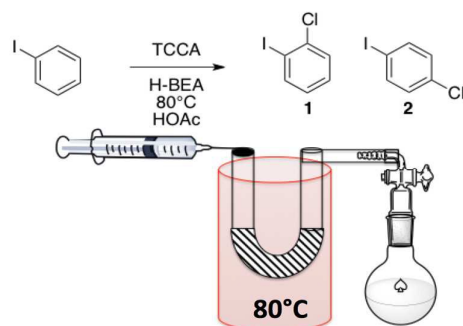


**Figure 2.** Continuous-flow synthesis of chloroarenes.

### 3. Results discussion

Commercial catalysts were evaluated in the benchmark chlorination reaction of iodobenzene in order to find an optimal heterogeneous catalyst. Those catalysts are characterised in Table 1 (general screening).

**Table 2.** Screening of the catalysts. Data obtained after 1h of reaction at 80°C.

Entry	Catalyst	Conversion [%]	S(Mono-chlorinated products) [%]	S( <i>para</i> -product) [%]	S( <i>ortho</i> -product) [%]
1	-	2	0	0	0
2	AlCl <sub>3</sub>	28	84	46	38
3	H <sub>2</sub> SO <sub>4</sub>	80	88	44	44
4	H-ZSM-5 (13)	20	68	42	26
5	H-ZSM-5 (25)	11	71	53	18
6	H-MOR (Zeolyst)	21	89	50	39
7	H-USY (Zeolyst)	72	92	49	43
8	H-Y (Aldrich)	66	92	52	40
9	H-EMT (UOP)	49	86	49	37
10	Cs <sub>2</sub> HPW <sub>12</sub> O <sub>40</sub>	4	84	45	39
11	H-*BEA (Zeochem)	71	97	58	39

Reaction conditions: 1 mmol iodobenzene, 0.33 mmol TCCA, 100 mg zeolite at 80°C, 1h, 5 mL DCE. Conversions were calculated based on the disappearance of the reactant. Selectivities are determined after corresponding calibration.

In the general screening, various acid site densities, pore sizes and topologies as well as crystal sizes were compared (Table 1). \*BEA zeolite (entry 11, Table 2) appeared as the most promising

candidate, leading to a 71% iodobenzene conversion and extremely high 97% selectivity in monochlorination products. Therefore, as it will be presented below, different kinds of \*BEA zeolites were prepared and compared for this reaction.

It is worthy to mention that in the absence of catalyst almost no reaction occurred (entry 1). In contrast, homogeneous Lewis and Brønsted acids led to medium and high iodobenzene conversions (entries 2-3). Especially, sulphuric acid efficiently catalysed this chlorination reaction (80% conversion with a 88% selectivity). This result is in agreement with earlier studies.<sup>8,9</sup> However, no special regioselectivity can be observed as a 1 to 1 *ortho-para*-chloriodobenzene mixture was produced (entry 3). This result corresponds to the thermodynamical product distribution in the absence of any zeolite related shape selectivity. Brønsted solid acids led to significant variations in conversions and selectivities, which is obviously linked to their intrinsic properties: acid site density, pore topology, crystal size and specific surface area (entries 4-9).

C<sub>2</sub>HPW<sub>12</sub>O<sub>40</sub> heteropolyacid with a high S<sub>BET</sub> of 123 m<sup>2</sup>.g<sup>-1</sup> remains almost inactive (entry 10) indicating that a dispersed Brønsted acidity is not sufficient to perform the halogenation. Medium-pore sized ZSM-5 zeolites led to conversions in the 11-20% range, proportional to the acid site density. Interestingly, the selectivity in monochlorination products seems to be independent from the conversion. Larger pore zeolites (entries 7-9) allowed to achieve higher conversions, *i.e.*; 72, 66 and 49 % for H-USY, H-Y and H-EMT, respectively. These results are in agreement with former studies which highlighted a better performance of USY and EMT zeolites for nitrobenzene chlorination.<sup>16a,c,e</sup> Surprisingly, only 21% conversion could be achieved over H-MOR which may also indicate a fast deactivation in 1D zeolite pores (entry 6).

**Table 3.** Characterisation of \*BEA zeolites.

Entry	Catalyst	Si/Al Global <sup>a</sup>	Si/Al Framework <sup>b</sup>	n(H <sup>+</sup> ) [mmol H <sup>+</sup> /g <sub>catalyst</sub> ] <sup>c</sup>		S <sub>BET</sub> [m <sup>2</sup> /g]	V <sub>μ</sub> [cm <sup>3</sup> /g]	V <sub>meso</sub> [cm <sup>3</sup> /g]	Crystal size [nm]
				Brønsted	Lewis				
				1	*BEA				
2	*BEA NC	15	23	0.44	0.34	726	0.24	0.71	40
3	*BEA MC	14	23	0.62	0.11	626	0.23	0.05	5000
4	*BEA NS	17	22	0.13	0.18	977	0.30	0.74	< 50

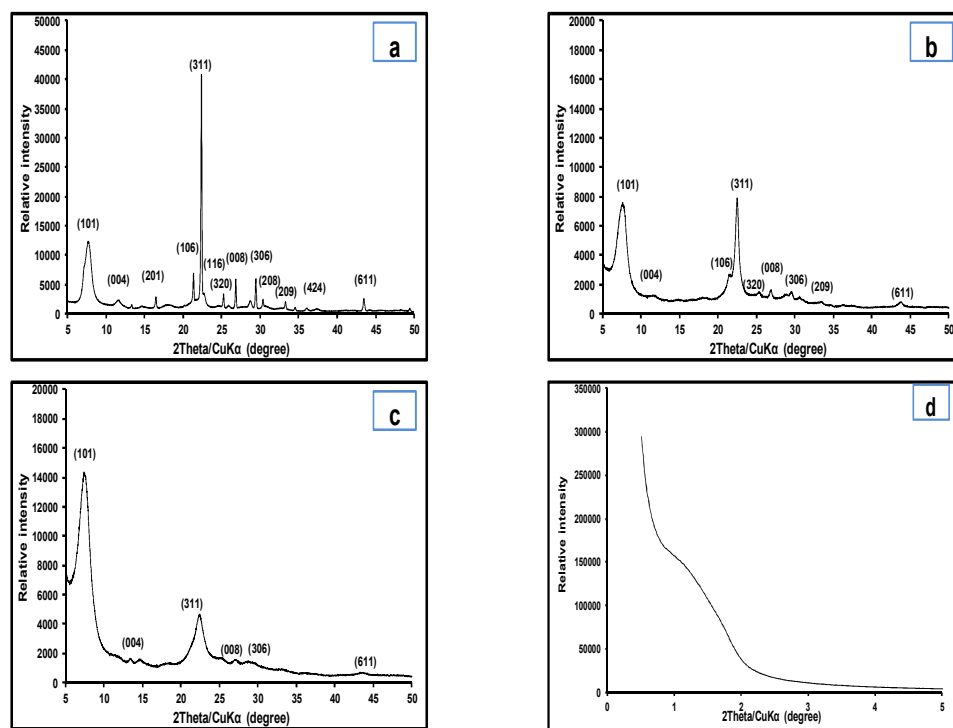
<sup>a</sup> measured by XRF ; <sup>b</sup> drawn from T-O-T band at 1080-1200 cm<sup>-1</sup> using the correlation given in <sup>25</sup>; <sup>c</sup> Acid sites determined by integrating and normalizing Py-absorption bands at 1540 and 1455 cm<sup>-1</sup> ; <sup>d</sup> Values taken from<sup>26</sup>.

Interestingly, the highest selectivity towards targeted products was achieved over commercial \*BEA zeolite. This interesting result led us to focus on series of rationally designed \*BEA zeolites (Table 3). According to the characterisation studies, those data show that the three different zeolites obtained exhibit similar Si/Al ratios but significantly differ in crystal size. Consequently, major

differences are observed in terms of textural properties: external surface areas ( $S_{\text{BET}}$  ranging from 560 to 977  $\text{m}^2\cdot\text{g}^{-1}$  in entries 1 and 4 in Table 3), porosities which may ‘a priori’ impact the diffusion of the reactants and products throughout the zeolite frame. It is important to note that the commercial zeolite \*BEA is very similar to the NC sample which will be confirmed below by the characterisation but as well in the catalytic behaviour.

As-prepared \*BEA zeolites: micro-crystal (MC), nano-crystal (NC) and nano-sponge (NS) samples were thoroughly characterised by XRD, XRF,  $\text{N}_2$  adsorption, SEM, TEM and FTIR. Their main features are summarized in Table 3 and Figures 3 and 4. Additional characterisation of these materials can be found in the recent study dealing with their use in the ethanol-to-hydrocarbons reaction.<sup>21</sup>

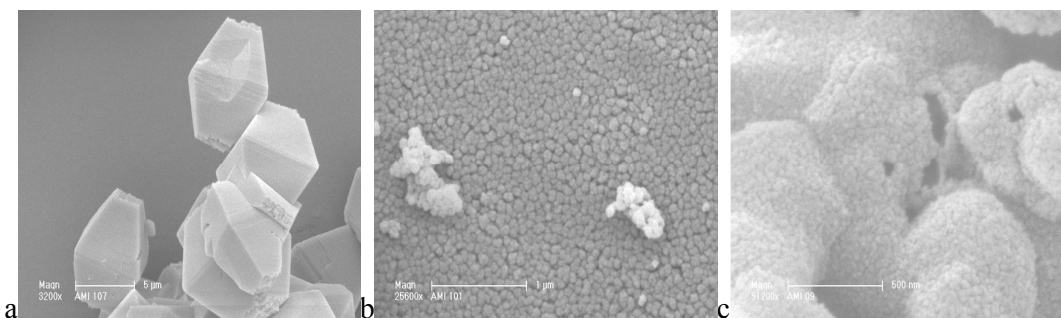
The XRD patterns of the three calcined samples are presented in Fig. 3. Whatever the synthesis protocol, the only crystalline phase formed remains \*BEA. For the NC and NS samples, the reflections are both far less intense and broader than the intensities found in MC sample, probably due to a smaller crystal size. For the NS sample, a broad peak in the low-angle region of the XRD pattern reveals a quite ordered mesoporosity (Fig.3d).



**Figure 3.** XRD patterns of calcined a) micron-sized \*BEA, b) nano-sized \*BEA and c) nano-sponge \*BEA, d) Low angle XRD pattern of calcined \*BEA nanosponges.

SEM images for the three samples are given in Fig.4. SEM micrograph of MC crystals prepared in the presence of TEAOH exhibits the characteristic truncated bipyramidal shape of beta

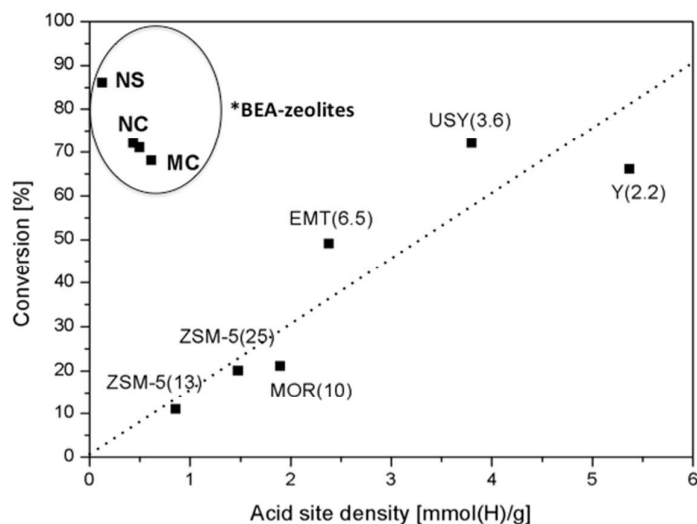
zeolite with crystal sizes ranging from 6 to 10  $\mu\text{m}$ .<sup>27</sup> Pseudo-spherical crystals with an average size of 40 nm are observed for the NC sample. \*BEA NS sample, synthesised from a poly-quaternary ammonium surfactant ( $\text{N}_{4\text{-phe}}$ ), exhibits a sponge-like morphology with nano-sized zeolite particles (Figure 4c). TEM micrographs demonstrated a somewhat ordered inter-crystallite mesoporosity for NS sample as compared to the NC sample.<sup>21</sup>



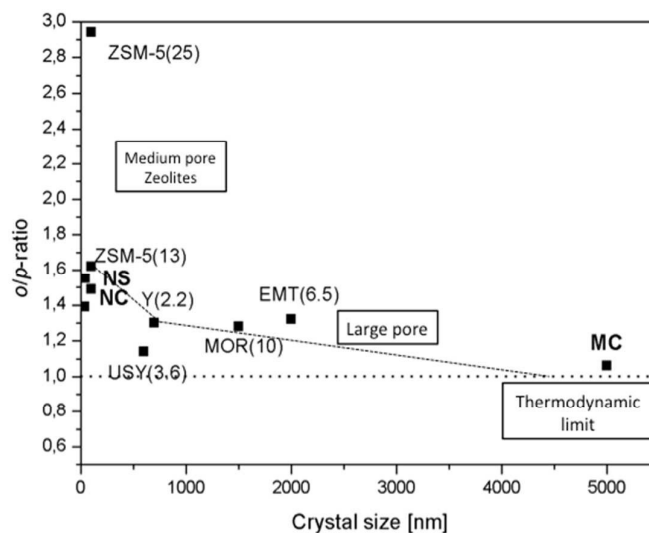
**Figure 4.** SEM micrographs of different \*BEA zeolites a) MC, b) NC and c) NS.

Figure 5 presents the conversion of iodobenzene which seems to be related to the acid site density, except for the investigated \*BEA-zeolites. Indeed, the \*BEA framework topology may provide a peculiar spatial arrangement, where an optimum can be found. Indeed, this seems to be achieved between a molecular diffusion inside the porous network and the acid site density. \*BEA zeolite displays two types of 12 membered-ring channels having 0.66 x 0.67 and 0.56 x 0.56 nm, respectively. Iodobenzene exhibits a  $\text{C}_{2v}$  symmetry with a C-I bond length of 0.21 nm.<sup>31</sup> The size of the aromatic ring fits well in the [001] channels (0.56 nm). Furthermore a non-flat diffusion is also possible at the channel intersections or in close to 0.7 nm-sized [100] channels for iodobenzene.

The studied reaction is an electrophilic aromatic substitution comparable to Friedel Crafts acylations for which \*BEA zeolites are reportedly very competitive catalysts.<sup>28</sup> Figure 6 then, presents the *o/p*-ratio of the benchmark reaction as a function of the crystal size of the different tested zeolites, shows that \*BEA zeolite's medium sized pores favour the production of para-substituted aromatics, large crystals, however, leading to long residence times, favour the production of the thermodynamically favoured 1/1 *p/o*-mixture.



**Figure 5.** The conversion of the benchmark reaction seems to be related to the acid site density, except for the different \*BEA-zeolites.



**Figure 6.** The *o/p*-ratio as a function of the crystal size, large crystals exhibit long residence times which favour the production of thermodynamically favoured 1/1 *o/p*-mixture.

It is therefore worthy to mention that this relatively high para-selectivity can be attributed to a special confinement of iodobenzene molecules within [100] and [001] \*BEA channels, thus inducing improved adsorption/desorption steps on fewer acid sites with respect to FAU structure. Similar spatial confinement has already been reported for bromination reactions in single-wall carbon nanotubes having a diameter of 0.7 nm.<sup>32</sup>

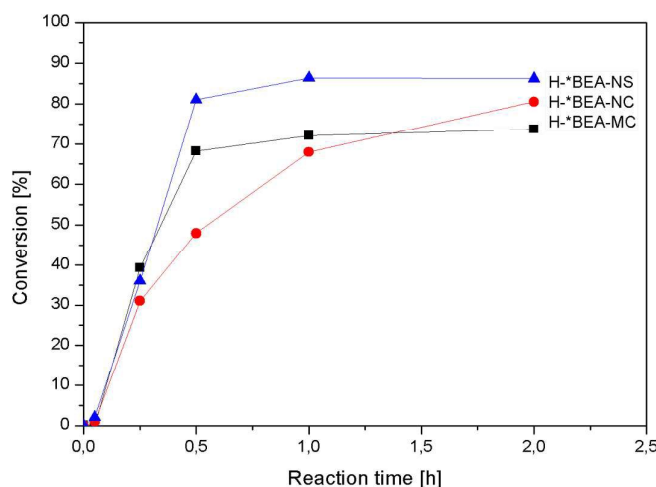
**Table 4.** Catalytic data collected for \*BEA-zeolites in the chlorination of iodobenzene.

Entry	Catalyst	Conversion [%]	S(mono-chlorination) [%]	S( <i>para</i> ) [%]	S( <i>ortho</i> ) [%]	TOF [ $\text{mol}_{\text{Iodobenzene conv.}} / \text{mol}_{\text{H}^+} \cdot \text{1/h}$ ] <sup>a</sup>
1	H-*BEA	71	98	58	39	15.2
2	H-*BEA MC	72	97	50	47	11.6
3	H-*BEA NC	68	98	57	41	15.5
4	H-*BEA NS	86	97	59	38	66.2

reaction conditions: 1 mmol iodobenzene, 0.33 mmol TCCA, 100 mg zeolite at 80°C, 1h, 5 mL DCE.

Conversions were calculated based on the disappearance of the reactant. Selectivities were determined after corresponding calibration. a: TOF were calculated after 60 min of reaction.

Table 4 shows the performances of these different \*BEA zeolites. The design of \*BEA zeolites is indeed possible since one can observe an improvement in conversion after 60 min reaction time (from 68 up to 86%). Likewise, a strong impact on TOF values could be evidenced *i.e.*; up to 9 times higher over the nanosponge beta zeolite compared with the commercial zeolite. The general trend for these TOF values is the following: \*BEA NS > NC = commercial \*BEA > MC (Table 4) which is a sound indication of a positive impact of hierarchical ordered porosity on the catalytic properties of \*BEA zeolites. This is supported by the fact that \*BEA NC and NS zeolites exhibit high external  $S_{\text{BET}}$  values with respect to \*BEA MC sample.<sup>21</sup>

**Figure 7.** Reaction profile versus time of the batch chlorination of iodobenzene over different as-synthesised \*BEA zeolites.

The change in crystal sizes further impacted the catalyst activity (Figure 7), where a conversion limit of about 70% was achieved over MC sample, whereas nanosized samples further

converted iodobenzene suggesting that mass transfer limitations could hamper the reaction paths in \*BEA MC zeolite and favour deactivation due to pore blocking.

After studying these different beta zeolites and evidencing the huge potential of tailor-made zeolites for improvement in this reaction if used at larger scale, our main goal now was to optimise the catalytic reaction in order to set-up an eco-compatible process. Based on the results and characterisation data, it is worthy to try to propose a "greener" halogenation process. In the following part, the cheapest (commercial zeolite) was chosen for an optimisation of the reaction conditions: solvent, scope of the reaction and lastly the development of a continuous process.

**Table 5.** Screening of solvents for the iodobenzene chlorination reaction.

Entry	Solvent (pK <sub>a</sub> )	Conversion [%]	S(Mono-chlorinated products) [%]	S( <i>para</i> -product) [%]	S( <i>ortho</i> -product) [%]
1	1,2-DCE	48	98	58	38
2	DMF	0	0	0	0
3	MeCN	84	93	45	48
4 <sup>a,b</sup>	Toluene	44	0	0	0
5 <sup>b</sup>	H <sub>2</sub> O (15.7)	85	71	39	31
6 <sup>b</sup>	2-propanol (16.5)	43	23	15	7
7 <sup>b</sup>	AcOEt	56	54	25	28
8	-	49	97	51	47
<b>9</b>	<b>AcOH</b>	<b>100</b>	<b>83</b>	<b>47</b>	<b>36</b>
10 <sup>c</sup>	AcOH	48	9	4	3
11 <sup>d</sup>	TFAOH (0.23)	99	92	43	45
12 <sup>d</sup>	HCOOH (3.77)	96	91	53	38
13 <sup>d</sup>	AcOH (4.76)	68	96	63	34

reaction conditions: 1 mmol iodobenzene, 0.33 mmol TCCA, 100 mg H-\*BEA corresponding to 0.05 mmol H<sup>+</sup> (5 mol-%) at 80°C, 30 min, 5 mL solvent. Conversions were calculated based on the disappearance of the reactant. Selectivities are determined after corresponding calibration (Fig. S2).

a: toluene in excess as compared to iodobenzene is chlorinated, iodobenzene degrades.

b: low monochlorination selectivities are due to both iodobenzene degradation for instance to form chlorobenzene or di-/tri-chlorination.

c: blank experiment without H-\*BEA.

d: same reaction conditions than in entry 9, but to compare the different carboxylic acids these tests have been carried out at room temperature 25°C in order to evidence a link between the pK<sub>a</sub> of the solvent and the solvent-catalyst activity.

A solvent screening, from apolar aprotic to polar and protic, was undertaken taking into account GSK's expanded solvent selection guide.<sup>29,30</sup> Interestingly, acetic acid a sustainable and non-

toxic solvent has proven to be the most promising for the reaction (Table 5). Indeed, it allows gaining in catalytic activity while a very high selectivity towards monochlorinated products could be maintained. As a weak Brønsted acid, acetic acid alone did not catalyse the reaction in the absence of a strong heterogeneous Brønsted acid (Entry 9, Table 5). Several other interesting trends could be drawn from this solvent screening. The reaction seems to perform better in protic polar solvents. In the case of toluene (Entry 4), the aromatic solvent was chlorinated, while iodobenzene suffered from halogen exchange forming chlorobenzene. The same phenomenon also occurred in 2-propanol and ethyl acetate (entries 4-7). A further set of experiments carried out at room temperature with different carboxylic acids ( $\text{CF}_3\text{COOH}$ ,  $\text{HCOOH}$  and  $\text{CH}_3\text{COOH}$  entries 11-13) underlines the link between the solvents  $\text{pK}_a$  and the activity of the considered solvent-catalyst system. Interestingly, at stronger acidities the reactions seem to be catalysed by the solvent itself since the *p/o*-ratio changes from 1.9 to 1.4 to 1 when comparing acetic acid to formic acid and to trifluoroacetic acid, respectively.

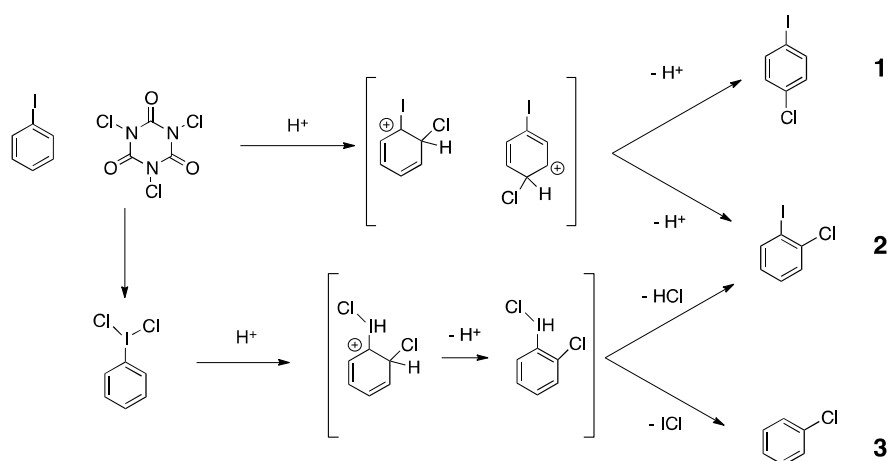


**Figure 8.** Proposed reaction mechanism leading to the observed by-products distribution

While chlorination reactions of aromatics with chlorine gas in apolar aprotic solvents tend to involve radicals, in acetic acid with a Brønsted acid catalyst the ionic pathway is more plausible (Figure 8). Depending on the solvent and the zeolite used, we observed an undesired reaction leading to the formation of chlorobenzene (up to 10% in selectivity). The earlier mentioned side reaction of the halogen exchange may occur through the intermediate formation of iodobenzenedichloride, which subsequently decomposes in contact with a zeolite to form chlorobenzene or *ortho*-substituted chloriodobenzene. Several tests have been performed to support this tentative explanation: when iodobenzene was in contact with TCCA (with or without zeolite), one was to detect iodobenzenedichloride by  $^1\text{H-NMR}$  and  $^{13}\text{C-NMR}$  (Fig.S3-S6). In addition, a yellow coloration of the reaction mixture could be observed suggesting the presence of  $\text{PhICl}_2$  and  $\text{ICl}$ . In the case of zeolite-catalysed reaction, chlorobenzene could be detected by gas chromatography. In contrast, for the chlorination of bromobenzene, which should not form bromobenzenedichloride intermediates, the

halogen exchange reaction, thus the formation of chlorobenzene could not be observed. Furthermore no coloration of the reaction mixture could be observed.

After finding optimal reaction conditions for our benchmark reaction, we steered our focus on the extension of the reaction scope. Various substituted aromatics were submitted to those optimal conditions. For comparison, several other halogenating agents were also investigated (Table 6).

With TCCA, the monochlorination was achieved for all arenes, except with strongly deactivated nitrobenzene (entry 6). As *'a priori'* expected, a classical trend was observed with more electron-rich aromatics led to higher conversions (Entries 5, 8 and 9). The un-functionalised and cheapest aromatic benzene was quite successfully converted to the corresponding iodo-, bromo- or chlorobenzenes (entries 1, 12 and 13). It is of utmost importance to note that these compounds could be obtained very selectively (91-100%) in their mono-halogenated forms and that non converted aromatics may be re-cycled in a continuous flow set up at a larger scale. Rewardingly, the cheaper TCCA is a better chlorinating agent both in terms of activity and selectivity than NCS (entries 1 vs 10 and 5 vs 9). Using NBS and NIS as brominating or iodinating agent the reaction also proceeds at room temperature with low to modest conversion (entries 11-15).

**Table 6.** Scope of H-\*BEA-catalysed chlorination reaction.

Entry	Reactant 	T [°C]	Halogenating reactant (equiv.)	Conversion [%]	S(Mono-chlorinated products) [%]	S( <i>para</i> -product) [%]	S( <i>ortho</i> -product) [%]
1	R= H	80	TCCA (0.33)	44	91	-	-
2	R = Me	80	TCCA (0.33)	66	98	73	25
3	R = Cl	80	TCCA (0.33)	38	100	58	40
4	R = Br	80	TCCA (0.33)	48	100	52	48
5	R = I	80	TCCA (0.33)	100	83	59	39
6	R = NO <sub>2</sub>	120	TCCA (0.33)	< 5	100	-	-
7	R = NH <sub>2</sub>	80	TCCA (0.33)	61	84	37	59
8	R = OMe	80	TCCA (0.33)	89	100	79	21
9	R = I	80	NCS (1)	56	80	45	35
10	R = H	80	NCS (1)	26	2	-	-
11	R = H	20	NBS (1)	18	100	-	-
12	R = H	80	NBS (1)	40	76	-	-
13	R = H	20	NIS (1)	37	100	-	-
14	R = H	80	NIS (1)	86	89	-	-
15	R = H	20	I <sub>2</sub> (1)	< 5	100	-	-

reaction conditions: 1 mmol aromatic, 1 equiv. Halogen, 100 mg H-\*BEA corresponding to 0.05 mmol H<sup>+</sup> (5 mol-%) at 80°C, 30 min, 5 mL acetic acid. Conversions were calculated based on the disappearance of the reactant. Selectivities are determined after corresponding calibration.

Unfortunately, at higher temperatures the high selectivity towards monohalogenated products decreases (entries 11 vs. 12 and 13 vs. 14), when compared to reactions carried out at room temperature. The reaction with molecular iodine did not lead to significant degree of conversion (entry 15).

For large scale applications, selectivity plays a crucial role whereas conversion limitations can be overcome by recycling unconverted reactant. This is of special interest when applied in a flow process. Therefore, we performed a recyclability test for our system: commercial \*BEA zeolite exhibited a limited loss in activity after 10 reaction cycles, whereas \*BEA NS zeolite deactivated much faster (Figure 9). This might be due to its higher specific surface area, thus adsorbing more water or other detrimental molecules which cannot be removed between consecutive runs. In addition, the short crystal thickness of \*BEA NS zeolite, combined with its low acidity, may limit the growth of coke molecules as well as their accumulation inside micropores. In other reactions, however, in the ethanol-to-gasoline process for instance, the extreme downsizing of zeolite crystal led to an unexpected pore blocking.<sup>21</sup>

It is noteworthy that, after calcination the activity as well as the selectivity could be completely re-established for both catalysts, reinforcing the earlier mentioned hypothesis for deactivation.

Lastly, both promising nano-sized \*BEA zeolites were applied to a continuous flow set-up (Figure 9). Although \*BEA-NS seems to deactivate more rapidly in consecutive batch reactions, it is very tolerant and resistant to the flow set-up. Indeed, no different behaviour compared to the \*BEA-NC sample could be noticed. The parameters of the continuous flow process were set to feed the same iodobenzene quantity found after 12 consecutive runs under batch conditions. A molar hourly space velocity of  $61 \text{ mmol(arene).(g(catalyst).h)}^{-1}$  was applied for this optimised reaction. Compared with our early semi-continuous gas-solid set-up exhibiting a molar hourly space velocity  $1.7 \text{ mmol(arene).(g(catalyst).h)}^{-1}$ ,<sup>16b</sup> this new continuous liquid-solid process can produce more than 30 times faster a desired halogenated arene. Interestingly, both zeolites seem more resistant toward deactivation under flow operations. Under these conditions, 100 kg iodobenzene may be converted per  $\text{kg}_{\text{cat}}$  in a single day.

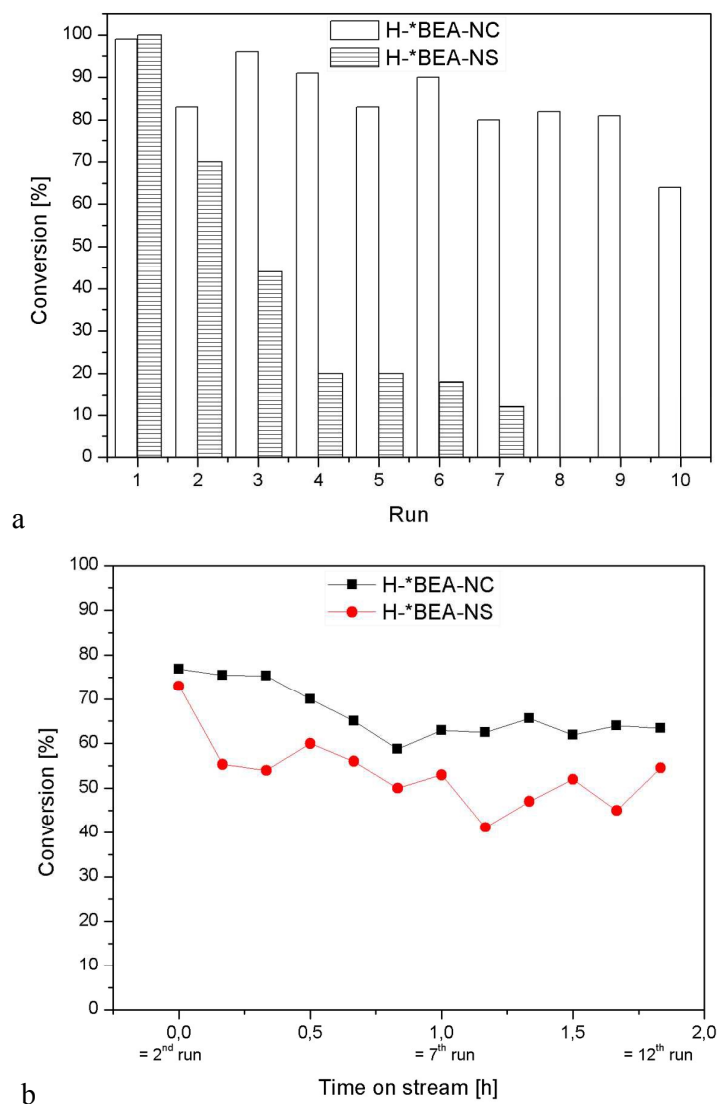


**Figure 9.** a) recycling experiment with commercial \*BEA-zeolite: 30 min of reaction. recycling with \*BEA-NS-zeolite: 30 min of reaction and b) continuous flow chlorination of iodobenzene corresponding to 12 runs under batch conditions.

Finally, a dependence between the solid acid pore structure, more precisely \*BEA textural properties, and activity / selectivity in chlorination reaction could be established. Further studies are under progress to design a cost efficient flow process.

#### 4. Conclusion

Eco-compatible iodobenzene halogenation reaction by trichloroisocyanuric acid has been developed, which allowed a conversion superior to 95%, with nearly 100 kg iodobenzene converted per kg<sub>cat</sub> in a single day.

H-\*BEA zeolites were found the most performant catalysts among several solid acids and zeolite structures. According to thorough characterisation (microscopy, H/D exchange, BET, XRD), structure-activity relationships could be established for various synthetic \*BEA zeolites. Nano-sized \*BEA zeolites and more specifically nanosponge-like \*BEA crystals exhibited the highest catalytic performances with a conversion up to 100%, corresponding to TOF values of 66 h<sup>-1</sup> and a selectivity in monochlorinated products up to 98 %.

The main outcome of this study relies on the ability to set-up an eco-compatible continuous flow halogenation process catalysed by zeolites (Figures S7 and S8).

### Acknowledgements

PL would like to thank the National Research Fund Luxembourg (NRFL) for his PhD-grant (5898454).

---

<sup>1</sup> (a) H.-G. Franck and J.W. Stadelhofer, *Industrial Aromatic Chemistry*, Springer-Verlag, Berlin, Heidelberg, 1988, pp 224–226; (b) J.I. Kroschwitz, M. Howe-Grant, C.A. Treacy and L.J. Humphreys, *Encyclopedia of Chemical Technology*, vol. 6, Wiley, New York, 1993, pp 109–113.

<sup>2</sup> U. Beck and E. Löser, *Chlorinated Benzenes and other Nucleus-Chlorinated Aromatic Hydrocarbons*, Ullmann's Encyclopedia of Industrial Chemistry, Wiley-VCH, Weinheim, 2012.

<sup>3</sup> (a) "Chlorobenzene: *Webster's Timeline History*, 1851 - 2007", 2010, ICON Group International, Inc.; (b) <http://www.icis.com/resources/news/2005/12/02/570444/chemical-profile-chlorobenzene/> ICIS Chemical Business (02 December 2015 12:51)

<http://www.icis.com/resources/news/2005/12/02/570444/chemical-profile-chlorobenzene/>

<sup>4</sup> (a) C.-C. Chang, H. Je Cho, J. Yu, R. J. Gorte, J. Gulbinski, P. Dauenhauer and W. Fan, *Green Chem.* 2015, 174, 769 (b) C.-C. Chang, S. K. Green, C. L. Williams, P. J. Dauenhauer, W. and Fan, W. *Green Chem.* 2014, 16, 585. (c) X. Zhang, Z. Wang, K. Xu, Y. Feng, W. Zhao, X. Xu, Y. Yan and W. Yi, *Green Chem.* 2016, DOI: 10.1039/x0xx00000x

<sup>5</sup> H.-G. Franck and J.W. Stadelhofer, *Industrial Aromatic Chemistry*, Springer-Verlag, Berlin, Heidelberg, 1988, pp. 218–220.

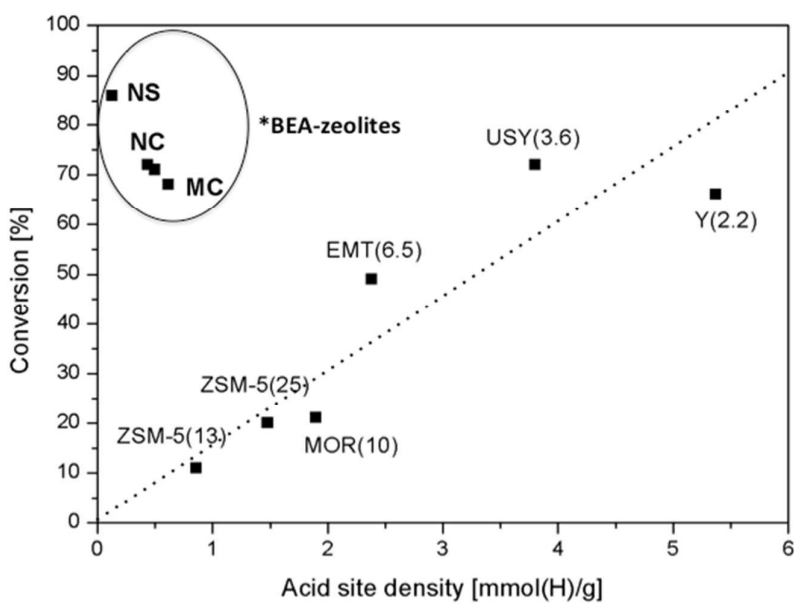
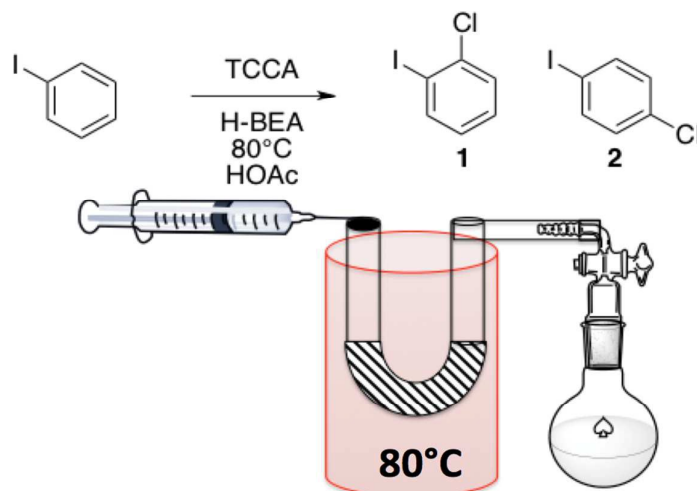
<sup>6</sup> E. Ram, *Krishna's new concepts in organic chemistry*, Krishna Prakashan media, 2007, pp 251.

<sup>7</sup> (a) K. Smith, M. Butters, W.E. Paget, D. Goubet, E. Fromentin and B. Nay, *Green Chem.* 1999, **1**, 83–90; (b) G.K.S. Prakash, T. Mathew, D. Hoole, P.M. Esteves, Q. Wang, G. Rasul and G.A. Olah, *J. Am. Chem. Soc.* 2004, **126** 15770–15776; (c) G.F. Mendonca, R.R. Magalhaes, M.C.S. de Mattos and P.M. Esteves, *J. Braz. Chem. Soc.* 2005, **16**, 695–698.

<sup>8</sup> (a) G. F. Mendonça, H. C. Sindra, L. S. de Almeida, P. M. Esteves and M. C. S. de Mattos, *Tetrahedron Lett.* 2009, **50**, 473–475; (b) L. S. de Almeida, P. M. Esteves and M. C. S. de Mattos, *Tetrahedron Lett.* 2009, **50**,

- 3001–3004; (c) R. S. Ribeiro, P. M. Esteves and M. C. S. de Mattos, *Tetrahedron Lett.* 2007, **48**, 8747–8751; (d) L. R. Sodr , P. M. Esteves and M. C. S. de Mattos, *J. Braz. Chem. Soc.* 2013, **24**, 212–218.
- <sup>9</sup> (a) G.F. Mendonca and M.C.S. de Mattos, *Quim. Nova.* 2008, **31**, 798–801; (b) S.D.F. Tozetti, L.S. de Almeida, P.M. Esteves and M.C.S. de Mattos, *J. Braz. Chem. Soc.* 2007, **18**, 675–677; (c) G.F. Mendonca, A.M. Sanseverino and M.C.S. de Mattos, *Synthesis.* 2003, 45–48; (d) G.A. Hiegel and K.B. Peyton, *Synth. Commun.* 1985, **15**, 385–392; (e) L. de Luca and G. Giacomelli, *Synlett.* 2004, 2180–2184; (f) L. de Luca, G. Giacomelli and G. Nieddu, *Synlett.* 2005, 223–226; (g) A. Shiri and A. Khoramabadi-Zad, *Synthesis* 2009, 2797–2801.
- <sup>10</sup> (a) U. Tilstam and H. Weinmann, *Org. Process Res. Dev.* 2002, **6**, 384–393; (b) G.F. Mendonça, M.C.S. de Mattos, *Curr. Org. Synth.* 2013, **10**, 820-836; (c) A.K. Mishra, H. Nagarajaiah and J.N. Moorthy, *Eur. J. Org. Chem.* 2015, 2733-2738.
- <sup>11</sup> (a) T. Tsubogo, H. Oyamada and S. Kobayashi, *Nature* 2015, **520**, 329–332; (b) H. P. L. Gemoets, Y. Su, M. Shang, V. Hessel, R. Luque and T. No l, *Chem. Soc. Rev.* 2015; (c) B. Gutmann, D. Cantillo, C. O. Kappe, *Angew. Chemie Int. Ed.* 2015, **54**, 6688-6728. (d) R. P. Jumde, C. Evangelisti, A. Mandoli, N. Scotti and R. Psaro, *J. Catal.* 2015, **324**, 25–31.
- <sup>12</sup> T.F. Degnan Jr. *Top. Catal.* 2000, **3**, 349-456.
- <sup>13</sup> (a) J. Weitkamp, *Solid State Ionics*, 2000, **131**, 175–188; (b) N.Y. Chen, W.E. Garwood and F.G. Dwyer, *Shape Selective Catalysis in Industrial Applications* Marcel Dekker, New York, Basel, 1989, pp. 203–204.
- <sup>14</sup> (a) P.A. Jacobs, M. Dusselier and B.F. Sels, *Angew. Chem. Int. Ed.* 2014, **53**, 8621–8626. (b) M. Dusselier, P. van Wouwe, A. Dewaele, P. A. Jacobs and B. F. Sels, *Science*, 2015, **349**, 78–80.
- <sup>15</sup> K. Smith and G. A. El-Hiti, *Green Chem.* 2011, **13**, 1579–1608.
- <sup>16</sup> (a) M. Boltz, M. C. S. de Mattos, P. M. Esteves, P. Pale and B. Louis, *Appl. Catal. A* 2012, **449**, 1–8; (b) M. Boltz, P. Losch, B. Louis, G. Rioland, L. Tzanis and T. J. Daou, *RSC Adv.* 2014, **4**, 27242; (c) T. J. Daou, M. Boltz, L. Tzanis, L. Michelin and B. Louis, *Catal. Commun.* 2013, **39**, 10–13; (d) P. Losch, A. Martinez Pascual, M. Boltz, S. Ivanova, B. Louis, F. Montilla Ramos and J.A. Odriozola, *CR Chimie* 2015, **18**, 324; (e) G. F. Mendonça, A. R. Bastos, M. Boltz, B. Louis, P. Pale, P. M. Esteves and M. C. S. de Mattos, *Appl. Catal. A* 2013, **460-461**, 46–51.
- <sup>17</sup> W. Kuran, *Coordination Polycondensation, in Principles of Coordination Polymerisation: Heterogeneous and Homogeneous Catalysis in Polymer Chemistry - Polymerisation of Hydrocarbon, Heterocyclic and Heterounsaturated Monomers*, John Wiley & Sons, Ltd, Chichester, UK. 2002.
- <sup>18</sup> N. Miyaura and A. Suzuki, *Chem. Rev.* 1995, **95**, 2457-2483.
- <sup>19</sup> A.P. Singh and S. B. Kumar, *Catal. Lett.* 1994, **27**, 171-176.
- <sup>20</sup> A.P. Singh and S. B. Kumar, *Appl. Catal. A* 1995, **126**, 27-38.
- <sup>21</sup> A. Astafan, M.A. Benghalem, Y. Pouilloux, J. Patarin, N. Bats, C. Bouchy, T.J. Daou and L. Pinard, *J. Catal.* 2016, **336**, 1-10.
- <sup>22</sup> C. Coutanceau, J. M. da Silva, M. F. Alvarez, F. R. Ribeiro and M. Guisnet, *J. Chim. Phys.* 1997, **94**, 765.
- <sup>23</sup> (a) B. Louis, S. Walspurger and J. Sommer, *Catal. Lett.* 2004, **93**, 81-84; (b) J.P. Tessonnier, B. Louis, S. Walspurger, J. Sommer, M.J. Ledoux and C. Pham-Huu, *J. Phys. Chem. B.* 2006, **110**, 10390-10395; (c) S. Walspurger and B. Louis, *Appl. Catal. A* 2008, **336**, 109-115; (d) B. Louis, A. Vicente, C. Fernandez and V. Valtchev *J. Phys. Chem. C* 2011, **115**, 18603-18610.

- 
- <sup>24</sup> M. Guisnet, P. Ayrault and J. Datka, *Polish J. Chem.* 1997, **71**, 1455.
- <sup>25</sup> C. Coutanceau, J. M. da Silva, M. F. Alvarez, F. R. Ribeiro and M. Guisnet, *J. Chim. Phys.* 1997, **94**, 765.
- <sup>26</sup> M.E. Sad, C.L. Padro and C.R. Apesteguía, *Appl. Catal. A* 2008, **342**, 40–48.
- <sup>27</sup> O. Larlus and V. Valtchev, *Microporous Mesoporous Mater.* 2006, **93**, 55.
- <sup>28</sup> G. Sartori and R. Maggi, *Chem. Rev.* 2006, **106**, 1077–1104.
- <sup>29</sup> R. K. Henderson, C. Jiménez-González, D. J. C. Constable, S. R. Alston, G. G. A. Inglis, G. Fisher, J. Sherwood, S. P. Binks and A. D. Curzons, *Green Chem.* 2011, **13**, 854.
- <sup>30</sup> (a) S. B. Phadtare and G. S. Shankarling, *Green Chem.* 2010, **12**, 458–462; (b) D. Prat, A. Wells, J. Hayler, H. Sneddon, C. R. McElroy, S. Abou-Shehada and P. J. Dunn, *Green Chem.* 2016, **18**, 288-296. DOI: 10.1039/C5GC01008DJ.
- <sup>31</sup> J. Brunvoll, S. Samdal, H. Thomassen, L.V. Vilkov and H.V. Volden, *Acta Chem. Scand.* 1990, **44**, 23-30.
- <sup>32</sup> S.A. Miners, G.A. Rance and A.N. Khlobystov, *Chem. Commun.* 2013, **49**, 5586.



Continuous iodobenzene chlorination reaction: experimental set-up and conversion - acid site density dependence.